Impact of ring torsion on the intrachain mobility in conjugated polymers

Magnus Hultell* and Sven Stafström†
Department of Physics, Chemistry and Biology, Linköping University, S-58183 Linköping, Sweden
(Received 8 November 2006; published 13 March 2007)

We have developed a fully three-dimensional model based on the solution of the time-dependent Schrödinger equation for studies of polaron mobility in twisted polymer chains. Variations in ring torsion angles along a conjugated polymer chain are shown to have a strong effect on the intrachain charge carrier mobility. An increase in ring torsion between two neighboring monomers can cause electron localization and then result in a transition of the type of transport from adiabatic polaron drift to nonadiabatic polaron hopping. In particular, we show the sensitivity for such a transition in the case of random variations in the ring torsion angles along a poly(phenylene vinylene) chain. The effective energy barrier associated with the change in torsion angle also depends on the applied electric-field strength, and by increasing the field strength a transition back to adiabatic transport can be obtained.

DOI: 10.1103/PhysRevB.75.104304 PACS number(s): 71.38.−k, 72.10.−d, 72.80.Le, 73.20.Mf

I. INTRODUCTION

Electronic and optoelectronic devices based on conjugated polymers have attracted much interest in recent years, particularly for use in applications such as full color organic light-emitting diode (OLED) displays, organic field-effect transistor (OFET) integrated circuits, and photovoltaic (PV) cells. At present the speed, heating, and power efficiency of these devices are all limited by the transportation of charge through the active organic layer(s)[1] and a detailed understanding of the basic properties that govern these processes is therefore essential for further material improvements. From a macroscopic point of view, electronic transport is described by the (local) electric-field-induced directional velocity component $\langle \mathbf{v} \rangle$ of the mobile charge carriers, superimposed on their random thermal motion as a time and ensemble average. This implies a dependence on charge carrier transport on the temperature T and the applied electric field $\mathbf{E}$.

In addition to these extrinsic dependencies, also the intrinsic electronic properties are of fundamental importance for the transport. These properties are strongly linked to the morphology of the material, and the electronic interactions, in particular the resonance integrals, are directly related to the conformation of constituent molecules.[2] The resonance integrals among the highest occupied molecular orbitals (HOMOs) and the lowest unoccupied molecular orbitals (LUMOs) of the individual molecules are responsible for the (small) band dispersion of the valence and conduction bands of the organic semiconductor that determines the low-temperature hole and electron mobility, respectively. Since the shape of these molecular orbitals are complex with several nodal planes, the transfer integrals between neighboring molecules are extremely sensitive even to very small molecular displacements. In the case of molecular solids, the fluctuation amplitude of the resonance integrals due to thermal motion could be of the same order of magnitude as the average value.[3] Such temperature-induced disorder in the intermolecular coupling could in fact account for the power-law dependence of the mobility on temperature often considered a fingerprint of band transport.[4] Since the fluctuations also bring about a dynamic localization of the charge carrier, these results help to bridge the formally conflicting evidence from spectroscopy of localized carriers with the bandlike temperature dependence of charge-carrier mobility in organic solids.

Within the bulk of conjugated polymers, the situation is somewhat more complex. Thermal motion still modulates the intermolecular resonance integrals, but due to the flexibility of the polymer backbone, it is also necessary to consider modulation of the intramolecular resonance integrals. The relevance of such effects can be seen from the more than 2 orders of magnitude higher mobility of holes observed in poly(9 9-dioctylfluorene) (PFO) when compared with that observed in poly[2-methoxy,5-(2′-ethyl-hexyloxy)-1,4-phenylene vinylene] (MEH-PPV),[5,6] the major difference between the two being the suppression of ring torsion motion in the former. Yu *et al.* developed a model which incorporates the fluctuations of phenylene ring torsion in the PPV derivatives.[7] With this model they could explain not only the difference in mobility but also the approximate Poole-Frenkel form of the field dependence of mobility observed in many pristine conjugated polymers. However, since the model ultimately relies on the solution of the steady-state master equation of the system, it cannot bring about detailed knowledge of the mesoscopic physics at hand. For this purpose, we have developed a method based on the coupled time-dependent Schrödinger equation and the equation of motion of the constituent atoms. This approach is particularly suitable when combined with a cost efficient Hamiltonian that enable simulations of large enough systems.

A simple yet accurate atomic resolved molecular Hamiltonian developed for conjugated systems is that used in the Su-Schrieffer-Heeger (SSH) model originally developed for quasi-one-dimensional systems.[8] In this work, we have expanded the model into three dimensions such that the modulation of resonance integrals caused by the torsion of rings around σ bonds may be incorporated. With the aid of this Hamiltonian, we have studied how fluctuations in this type of ring torsion affect the motion of charge carriers along a single polymer chain. These studies involve stochastic distributions of ring torsions as well as specific torsion angle defects. As a model system, we will use the poly(phenylene

vinylene) (PPV) chain. The methodology is presented in Sec. II, followed by the results in Sec. III, summary and conclusions in Sec. IV.

II. METHODOLOGY

Our methodology ultimately relies on the simultaneous numerical solutions of the time-dependent Schrödinger equation,

$$i\hbar|\dot{\Psi}(t)\rangle = \hat{H}_{\mathrm{el}}|\Psi(t)\rangle, \tag{1}$$

and the lattice equation of motion

$$M_i\ddot{\mathbf{r}}_i = -\nabla_{\mathbf{r}_i}\langle\Psi|\hat{H}|\Psi\rangle - \lambda\dot{\mathbf{r}}_i. \tag{2}$$

Here, $\hat{H}$ ($\hat{H}_{\mathrm{el}}$) is the (electronic) molecular Hamiltonian, $\mathbf{r}_i$ and M_i are the position and mass of the ith atom, respectively, and λ is a viscous damping constant appended to account for heat dissipating from the system. These calculations may readily be performed using state-of-the-art numerical differential equation solvers, provided that the wave function $|\Psi\rangle$ is expanded as a linear combination in known basis functions. To enable computations on large enough systems, we develop, as previously stated, an extended version of the SSH model.

Like its predecessor, the model rely on the validity of the $\sigma-\pi$ separability, i.e., that the σ electrons can be treated in the adiabatic approximation. The lattice energy part of the system Hamiltonian H_{latt} is therefore treated classically. Since geometrical changes in the molecule are expected to be small, the σ energy for bonds, bond angles, and torsion angles can be expanded to second order around the undimerized state to yield a lattice energy Hamiltonian on the form[9]

$$\hat{H}_{\mathrm{latt}} = \frac{K_1}{2}\sum_{i>j}{}'(r_{ij}-a)^2 + \frac{K_2}{2}\sum_{j}{}'(\phi_j-\phi_0)^2 + \frac{K_3}{2}\sum_{k}{}'(\theta_k-\theta_0)^2, \tag{3}$$

K_1, K_2, and K_3 being the harmonic force constants, a and ϕ_0 the reference bond length and bond angles of the undimerized system, and θ_0 the reference torsion angles, to be discussed subsequently in Sec. III. All primed summations run over nearest neighbors and involve, in Eq. (3), unique geometrical variables, r_{ij}, ϕ_j, and θ_k, only.[9] Note that this form resembles that of the covalent part of the classical force field potential energy[10] in the limit of small torsion angels.

The π electrons are treated within the tight-binding approximation. This resolves into computations including nearest-neighbor resonance integrals β_{ij} only. These may be carried out within the Mulliken approximation,[11] which estimates the resonance integral as proportional to the overlap integral S_{ij} by a constant k,

$$\beta_{ij} = kS_{ij}. \tag{4}$$

Using Slater-type atomic orbitals, Hansson and Stafström[12] derived an analytical expression for the overlap integrals between $2p$ atomic orbitals (AO's) $\mathbf{p}_{\pi,i}$ and $\mathbf{p}_{\pi,j}$ on sites i and j (of arbitrary directions) from the master formulas of Mulliken *et al.*,[13]

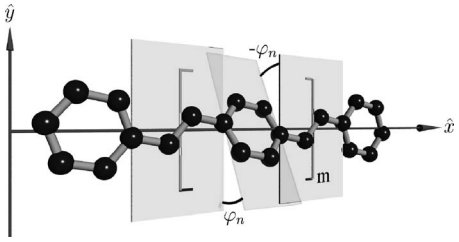

FIG. 1. The starting geometry of the poly(phenylene vinylene) chains are those of an undimerized system with two tail groups and M monomers, where the nth phenylene ring is twisted out of the xy plane, in which all vinylene bridges resides, by a torsion angle φ_n for $n \in [1, N]$.

$$S_{ij} = \cos(\Phi_{ij})\cos(\Omega_{ij})\cos(\Theta_{ij}) \times S_{2p\pi,2p\pi}(r_{ij}) - \sin(\Omega_{ij})\sin(\Theta_{ij}) \times S_{2p\sigma,2p\sigma}(r_{ij}), \tag{5}$$

where $\Phi_{ij} = \arccos(\mathbf{p}_{\pi,i}\cdot\mathbf{p}_{\pi,j}/|\mathbf{p}_{\pi,i}||\mathbf{p}_{\pi,j}|)$, $\Omega_{ij} = (\pi/2) - \arccos(\mathbf{p}_{\pi,i}\cdot\mathbf{r}_{ij}/|\mathbf{p}_{\pi,i}||\mathbf{r}_{ij}|)$, $\Theta_{ij} = -\Omega_{ji}$, and

$$S_{2p\pi,2p\pi}(r) = e^{-r\zeta}\left[1 + r\zeta + \tfrac{2}{5}(r\zeta)^2 + \tfrac{1}{15}(r\zeta)^3\right],$$

$$S_{2p\sigma,2p\sigma}(r) = e^{-r\zeta}\left[-1 - r\zeta - \tfrac{1}{5}(r\zeta)^2 + \tfrac{2}{15}(r\zeta)^3 + \tfrac{1}{15}(r\zeta)^4\right],$$

the orbital exponent ζ for the $2p$ orbitals of carbon being 3.07 Å^{-1}.[12] In planar systems $\mathbf{p}_{\pi,i}$ and $\mathbf{p}_{\pi,j}$ are always orthogonal to $\mathbf{r}_{ij}$ and, as a consequence thereof, all angles in $\{\Phi_{ij}\}$, $\{\Omega_{ij}\}$, and $\{\Theta_{ij}\}$ will be strictly zero. The $S_{2p\sigma,2p\sigma}$ term therefore vanishes, and since in this case there is no contribution from the π electrons to the σ-electron system, the $\sigma-\pi$ separability will not be jeopardized and Eq. (3) holds. This is the case also in the systems which we study, since the twisting of phenylene rings around the single bonds of the vinylene bridges (see Fig. 1) introduce nonzero terms only in $\{\Phi_{ij}\}$. For these systems, $\{\Phi_{ij}\}$ therefore span the complete set of torsion angles $\{\theta_k\}$ introduced in Eq. (3) and will be fully responsible for the modulation of the concerned overlap integrals $S_{2p\pi,2p\pi}$ by a factor of $\cos(\Phi_{ij})$ in accordance with Eq. (5). If expanded to first order around the undimerized state, the resonance integrals of Eq. (4) may then be written on the form

$$\beta_{ij} = \cos(\Phi_{ij})(\beta_0 - \alpha\Delta r_{ij}), \tag{6}$$

where

$$\beta_0 = kf(a) = A[15 + 15a\zeta + 6(a\zeta)^2 + (a\zeta)^3], \tag{7}$$

$$\alpha = kf'(a) = Aa\zeta^2[3 + 3a\zeta + (a\zeta)^2]. \tag{8}$$

Here, $A = k\,(e^{-a\zeta}/15)$ and $\Delta r_{ij} = (r_{ij} - a)$ is the bond-length distortion from the system with unidistant bond length a. This treatment is consistent with the one-dimensional SSH model,[8] since Eq. (6) naturally resolves in a linear approximation to β_{ij} on the form $\beta_0 - \alpha\Delta r_{ij}$ for planar molecules. It should be stressed though that Eqs. (7) and (8) impose a restriction on the ratio between β_0 and α through their mutual dependence on a, and although the parameters used for *trans*-polyacetylene in the original work of Su *et al.*[8] satisfies

this quotient, there are many examples in literature where this relation is violated.

In order to simulate charge transport, an electric field $\mathbf{E}_0$ is taken into account in the Coulomb gauge. The electric field is taken to be constant in time after a smooth adiabatic turn on. The total electronic Hamiltonian then reads

$$\hat{H}_{\mathrm{el}} = -\sum_{i>j}{}' \beta_{ij}(\hat{c}_i^\dagger \hat{c}_j + tc_i\hat{c}_j^\dagger) - e\sum_i \mathbf{r}_i\mathbf{E}_0\hat{c}_i^\dagger\hat{c}_i = \sum_{i,j}{}' \hat{c}_i^\dagger h_{ij}\hat{c}_j. \tag{9}$$

Finally, we note that the Hamiltonian should be supplemented with the constraint of fixed total bond length, i.e., $\Sigma'_{i>j}(r_{ij}-a)=0$, since a is the equilibrium lattice spacing of the undimerized system. Using the method of Lagrangian multipliers, it is simple to show that this restriction is incorporated into the model by subtracting a term in the "distance spring part" of the Hamiltonian,

$$\frac{K_1}{2}\sum_{i>j}{}'\left[(r_{ij}-a) - \frac{2\alpha}{K_1}\langle\cos(\Phi_{i'j'})\rho_{i'j'}\rangle\right]^2. \tag{10}$$

Having defined the constituent parts of the system Hamiltonian, the equation of motion may be readily derived by differentiating the total energy of the system with respect to the atomic coordinates $\mathbf{r}_i$, unraveling the interdependence with Eq. (1) through the density matrix elements $\rho_{ij}(t)$. If we make the ansatz that $\rho_{ij}(t)=\Sigma_p\psi_{ip}(t)f_p\psi^*_{jp}(t)$, where p is the molecular orbital (MO) index, $\psi_{ip}(t)$ the time-dependent MO, and $f_p\in[0,1,2]$ the time-independent occupation number of the pth MO, $\{\psi_{ip}\}$ will be solutions to the time-dependent Schrödinger equation

$$i\hbar\dot{\psi}_{ip}(t) = \sum_j h_{ij}(t)\psi_{jp}(t). \tag{11}$$

Solving Eqs. (2) and (11) simultaneously will thus provide the dynamics of charge-carrier transport through the system.

Naturally, the values of constituent parameters in this model are of major importance for the behavior of the system and must therefore be chosen so as to mimic that of a real PPV chain. For this purpose, we deployed the detailed procedure of relaxation of atomic positions[9] to a large number of parameter sets and compared the ground-state properties of these systems with those obtained from an *ab initio* calculation performed on an eight monomer long chain using B3LYP/6-31G^{**}. With a bond-length average of $a=1.4085$ Å, the *ab initio* conformation of the planar system is reproduced within an error margin of ~0.001 Å/bond for $k=11.04$, $K_1=37.0$ eV/Å, $K_2=70.0$ eV/rad^2, and $K_3=200.0$ eV/rad^2. Although this result is only weakly dependent on the later two parameters, a high value of K_3 was chosen so as to leave the intrachain torsion essentially static during dynamics simulations. This seems to be the relevant approximation (see below) for our study, since the dynamics of polaron transport occurs at a time scale which is considerably faster than the dynamics of phenylene ring torsion.[14]

III. RESULTS

The initial state conformation of the PPV chain in our dynamics simulations is that of an undimerized neutral system with torsion angles φ_n between the nth phenylene ring and its adjacent vinylene bridges (as illustrated in Fig. 1). These angles constitute the nonzero subset of $\{\theta_0\}$ in Eq. (3) and $\{\Phi_{ij}\}|_{t=0}$ in Eq. (7), but it should be stressed that since we are working with essentially static torsion, they are also fair approximations to those of the corresponding angles in $\{\theta_k\}$ and $\{\Phi_{ij}\}|_{t\neq 0}$. In a fashion reminiscent of that of simulated annealing, the polymer is then allowed to dynamically relax its atomic positions via dissipation of heat, and after roughly 140 fs it has acquired a stable ground-state configuration. In the case of a singly charged (one extra electron) polymer, which is the state of focus in this work, this corresponds to a polaron configuration. When the ground state is reached, the electric field is turned on and we monitor the nature and velocity of the polaron charge carrier as it propagates along the polymer chain. In order to span the full length of the system, the direction of the electric field is reversed when and if the charge carrier hits the chain end for the first time.

The first distribution of $\{\varphi_n\}$ that we consider is that for which the torsion of phenylene rings in the PPV chains are uniform, i.e., $\varphi_n=\varphi_0$ for $n\in[1,N]$, N being the number of phenylene rings in the system. Notably, this distribution comprise the planar ground-state system of PPV ($\varphi_0=0°$), whose properties we shall use as a reference for subsequent simulations on chains with randomly distributed phenylene ring torsion. Following the simulation procedure detailed above, we observe a continuous charge-density propagation accompanied by lattice distortions, characteristic of adiabatic polaron drift. From the time evolution of the charge density associated with the polaron, we obtain a constant velocity of propagation v for each value of φ_0, acquired once the polaron ceased to accelerate from the initial state of rest in systems of $N=51$.

These results enabled us to deduce the mobility $\mu=v/E_0$ as a function of φ_0 for $E_0=1.0\times10^4$ and 5.0×10^4 V/cm, respectively, as depicted in Fig. 2. The functional dependence observed closely resembles a $\cos^2(\varphi_0)$ modulation of the mobility of the planar system. Since according to Eq. (6), $\beta_n\propto\cos(\varphi_0)$, this implies that $\mu\propto\beta^2$. This is expected for nonadiabatic intermolecular transport in organic crystals,[15] but is clearly also a relevant description for the case of intramolecular adiabatic polaron drift. In accordance with earlier studies,[16] we also observe a lower limit in the resonance integral for which adiabatic transport can occur. This limit is shown to be reached at torsion angles of around 75° in the case of PPV. A uniform system with such high torsion angles has a total energy far above that of the planar ground-state configuration and is therefore very unlikely to exist in reality.

The velocity obtained in our simulations lies far above the sound velocity in the system, which with our choice of parameters is 0.11 Å/fs (the polaron velocity for a planar system, i.e., $\varphi_0=0$, is 4.32 Å/fs at $E_0=5.0\times10^4$ V/cm. Thus, the polaron velocity is supersonic. The decrease in mobility when the field strength is raised originates from the fact that

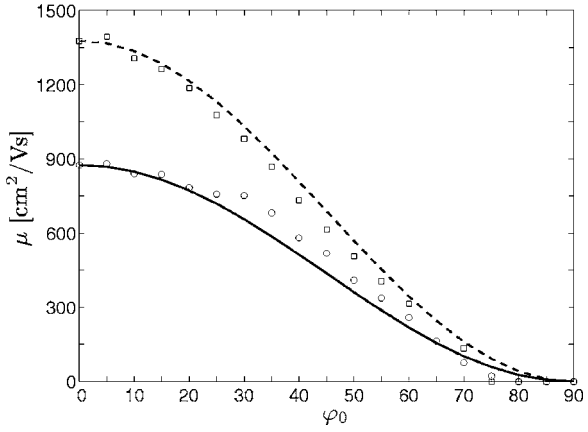

FIG. 2. The mobility $\mu=v/E_0$ as a function of uniform phenylene torsion angles φ_0 at field strengths $E_0=5.0\times10^4$ V/cm (circles) and $E_0=1.0\times10^4$ V/cm (squares) in PPV chains of size $N=51$. The solid and dashed lines display the dependence $\mu=\mu_0\cos^2(\varphi_0)$ with $\mu_0=\mu(\varphi_0=0°)$ for the high and the low field strengths, respectively.

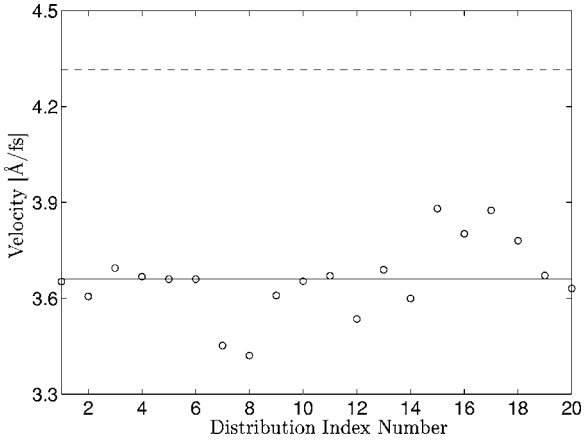

FIG. 3. The carrier velocities achieved in 20 $n=23$ systems, each subject to a rectangular distribution $[0,\varphi_u]$ of phenylene ring torsion angles ($\varphi_u=5°$), are indicated above with black circles. Also shown is the mean of these velocities (solid line) and the velocity attained in the completely planar system (dashed line). In all simulations, $E_0=5.0\times10^4$ V/cm.

the polaron velocity increases sublinearly with the field strength. This is an effect of a change in the effective mass, associated with the polaron with increasing (supersonic) velocities.[17]

As discussed above, the state with perfectly ordered phenylene ring torsion is probably rare in the amorphous phase of the polymer bulk. Steric effects related to disorder in the interchain distances can lead to a static distribution of $\{\varphi_n\}$ along the chain. Furthermore, even at low temperatures there are accessible phonon modes that involve phenylene ring torsion. Such modes lead to a dynamic behavior of the distribution of $\{\varphi_n\}$. In this work, we address the effect of a static disorder which then includes the disorder in the morphology (as well as a snapshot of the ring torsion phonon modes). From calculations of the vibrational spectrum of PPV oligomers, we can conclude, however, that the type of ring torsion vibrations shown in Fig. 1 has very low frequencies. The dynamics of polaron transport, at least in the adiabatic case, therefore occurs at a time scale, which is considerably faster than the dynamics of the ring torsion.[14] As discussed in Sec. II, the model is therefore such that the ring torsion angles are kept constant during the simulations, similar to the approach taken by, e.g., Troisi and Orlandi[4] for studies of intermolecular torsion.

The distribution function of $\{\varphi_n\}$ that we put into the simulations naturally has a large effect on the polaron dynamics. The function that correctly mimics the distribution of torsion angles in true bulk PPV is not available. We take as the next step in the investigations a truly stochastic distribution. Valuable insights in the limitations of the intrachain mobility in PPV chains can be gained by comparing our previous results for the ordered systems with those of the statistical average from simulations on systems with a rectangular distribution of phenylene ring torsion angles. Following the procedure detailed at the beginning of this section, we therefore conducted dynamics simulations on sets of 20 systems, each having $N=51$ phenylene rings with random rectangularly distributed torsion angles, i.e., $\varphi_n\in[0,\varphi_u]$, acquired by means of simple scaling from a uniform distribution $\{\chi_n\}\in[0,1]$ such that $\varphi_n=\chi_n\varphi_u$.

The charge-carrier velocities obtained for a set of distributions when φ_u is set to 5° are depicted in Fig. 3. Owing to the stochastic nature of φ_n, a constant velocity on monomer scale is no longer expected. The velocities are therefore obtained from a time-of-flight measurement over a region of 15 monomers along the PPV chain. As levels of reference, both the mean $\langle v\rangle$ of these time-of-flight (TOF) measurements (solid line) and the velocity attained within the completely planar system (dashed line) have been appended to Fig. 3. The results are striking; compared to the charge carrier velocity of the planar system, $\langle v\rangle$ decreased by 15% when $\{\varphi_n\}$ assumed a rectangular distribution with an upper limit torsion angle of $\varphi_u=5°$. This decrement in mobility is roughly 20 times larger than the decrement given by the maximum reduction of resonance integral, i.e., $1-\cos(5°)$, for all interatomic interactions in between phenylene rings and vinylene bridges. Considering also that the average value of phenylene ring torsion is only half of $\varphi_u=5°$ in systems with random distribution of $\{\varphi_n\}$, we may conclude that the impact of random distribution of ring torsion on the intrachain mobility in conjugated polymers is indeed significant.

Upon further increments of φ_u to 10° and 15°, corresponding to a maximum modulation of concerned resonance integrals amounts to 1.5% and 3.4%, respectively, there is a tendency of the systems to localize the density of charge to more than one region of the chain. It is then no longer meaningful to discuss transport in terms of an adiabatic polaronic charge carrier; rather the dynamics observed is best described as electron tunneling. The tunneling barriers correspond in this case to abrupt changes in the torsion angle from small to large values between neighboring monomer units. We will return to a more detailed discussion concerning this behavior below.

At even greater magnitudes of torsion, i.e. $\varphi_u=20°$, these barriers become so large that the wave function associated

with the charge carrier becomes completely localized. In this situation, the transport switches over to a nonadiabatic phonon-assisted hopping process.[18] The dynamics of this process is not captured by our model without inclusion of temperature. This lies outside the scope of this work and whenever we refer to such processes in the static phenylene ring torsion picture, it is made under the assumption that the only way for a completely localized polaron to propagate further through the system is with the aid of temperature fluctuations.

In order to better understand the mechanisms that govern charge-carrier transport, it is necessary to go beyond statistical averages and analyze in detail the dynamics of the individual systems. An example of such a system is represented in Figs. 4(a)–4(e). The bottom figure [Fig. 4(a)] shows the distribution of random numbers $\{\chi_n\}$ and the corresponding variations in the resonance integrals for $\varphi_u=15°$, whereas the other graphs [Figs. 4(b)–4(e)] show the net charge per monomer along the PPV chain as a function of simulation time for $\varphi_u=5°$, 10°, 15°, and 20°, respectively. All these simulations were carried out for $E_0=5.0\times10^4$ V/cm. In relation to these figures, it should be mentioned that the acquisition of the stable ground state, i.e., the first 140 fs, has been omitted and that the electric field, when turned on, points in the direction of decreasing monomer index. As mentioned above, the direction is reversed the first time that the polaron hits the chain end but not at the second bounce.

The signature of adiabatic polaron transport is evident in the cases of $\varphi_u=5°$ [Fig. 4(b)] and $\varphi_u=10°$ [Fig. 4(c)]. For $\varphi_u \geqslant 15°$, this picture changes quite dramatically and at $\varphi_u=20°$, the situation of localized wave functions discussed above is reached. The charge carrier is in this case initially localized in the region around monomers 5 and 6 [see Fig. 4(e)], in which the resonance integrals are large [c.f. gray bars in Fig. 4(a)]. This region is "terminated" by a rapid increase in the ring torsion angles at monomers 4 and 7, respectively. When the field is turned on, the potential in the region around monomers 10 and 11 becomes more favorable and the charge carrier can move through the relatively narrow barrier between these two regions. However, the polaron is, at the field strength of this simulation, unable to enter the wide region of larger torsion angles (larger values of $\{\chi_n\}$) in the right half of the system. Note that the tunneling barrier in terms of reduction of the resonance integral is as low as 6% which shows the sensitivity of adiabatic polaron transport to this type of disorder.

The case of $\varphi_u=15°$ corresponds to a state in between the adiabatic and nonadiabatic systems. Here, the charge carrier (as well as the geometrical deformation) is split into the two regions of small torsion discussed above. It is evident from the time scale that the motion across the system is considerably smaller in this case, but for this particular distribution of resonance integrals and for the given field strength, the carrier is able to travel through the system and contribute (adiabatically) to the current.

The dynamical behavior of the polaron moving in the "landscape" of varying torsion angles is of course dependent on the electric-field strength. The simulations presented in Fig. 4 are for $E_0=5.0\times10^4$ V/cm. Reducing E_0 to 1.0×10^4 V/cm will effectively prevent the carrier from being able to traverse the full length of the system even at $\varphi_u=5°$ and leaves it completely localized to the region centered at $n\in[10,11]$ already at $\varphi_u=10°$. This implies that

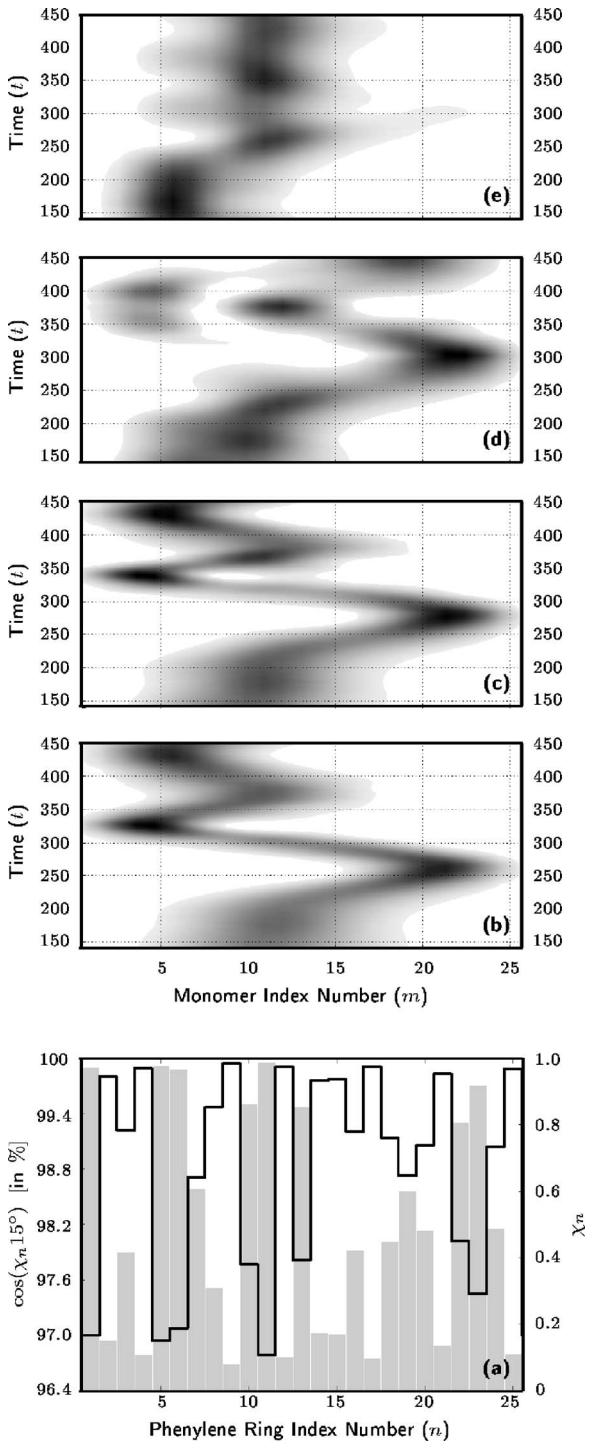

FIG. 4. The charge density as a function of time and position (for $E_0=5.0\times10^4$ V/cm) when incrementing the upper limit phenylene ring torsion angle φ_u to the rectangular distribution of $\varphi_n=\chi_n\varphi_u$ for a fix $\{\chi_n\}$ [the stair function in (a)] in steps of 5° from 5° to 20° is depicted in (b)–(e), with deeper levels of gray for higher density of charge. Also illustrated in (a) with light gray bars are the resonance integrals in between the phenylene rings and vinylene bridges when $\beta|_{\varphi_u=0°}$ is modulated by $\cos(\chi_n\varphi_u)|_{\varphi_u=15°}$.

superimposed on the disorder-induced transition from adiabatic to nonadiabatic transport, there also exists a field-induced transition from nonadiabatic to adiabatic transport. As a matter of fact, even though our model is not strictly one dimensional, the states are very sensitive to disorder in the resonance integrals and become localized even for small fluctuations in β. The effect of increasing the field strength is in this case to reduce the tunneling barriers between the states in the direction opposite to the field. With such very small barriers, the transport appears to be adiabatic as shown in Figs. 4(b) and 4(c).

We can conclude that the results from the simulations of the system with stochastic variations in the torsion angles gave valuable insights into how random disorder in the torsion angles affects the polaron transport properties. In particular, from Fig. 4, it is evident that rapid changes in torsion angles (and in β) are the main cause of localization. The sites where these changes occur act as barriers for polaron transport.

In order to obtain further insight into how such barriers affect the transport properties, we now turn to studies of well-defined barriers caused by torsion of specific phenylene rings in otherwise planar PPV chains. Three barrier parameters have been studied: (i) width, i.e., the number of consecutive rings subjected to torsion, (ii) height, i.e., the value of the torsion angle of a single ring, and (iii) the separation distance between two barriers. The studies of the barrier width were performed on a planar system in which one, two, and three neighboring phenylene rings in the central region of the chain were subject to uniform torsion. The studies were performed for a number of different torsion angles. Only the case of $\varphi=15°$ is shown in Fig. 5. This choice of torsion angle results in the desired crossover from delocalized to localized wave functions or from the case of adiabatic to nonadiabatic motion discussed above. For smaller torsion angels ($\varphi \leqslant 10°$), this transition does not occur and for larger angles ($\varphi \geqslant 20°$), the transition occurs already for a segment of one or two monomer units. The time evolution of the density of charge at $E_0=5.0\times10^4$ V/cm shows that the charge goes through the barrier of unit length, even though the barrier causes some disturbance of the density distribution, making the polaron more extended during the process of barrier crossing. The double ring barrier obviously causes stronger backscattering of the polaron and only a fraction of the charge can tunnel through the barrier. As time evolves, this fraction is again attracted to the region to the right of the barrier, where the majority of the charge density remains. The ground state of the system depicted in Fig. 5 is, of course, that with the polaron on the left side of the barrier since the electrostatic potential due to the external electric field is lower in this region, but the barrier prevents the polaron from moving there. We emphasize that these results are obtained for a particular value of E_0 and that an increasing field strength can result in crossing of the barrier.

The increase in the strength of the barrier by increasing the width can be converted in to a unit barrier length with increasing height. As it turns out, the field-induced time evolution of the density of charge for a system where the two and three center most phenylene rings have been twisted an angle of 15° [see Figs. 5(b) and 5(c)] looks very similar to

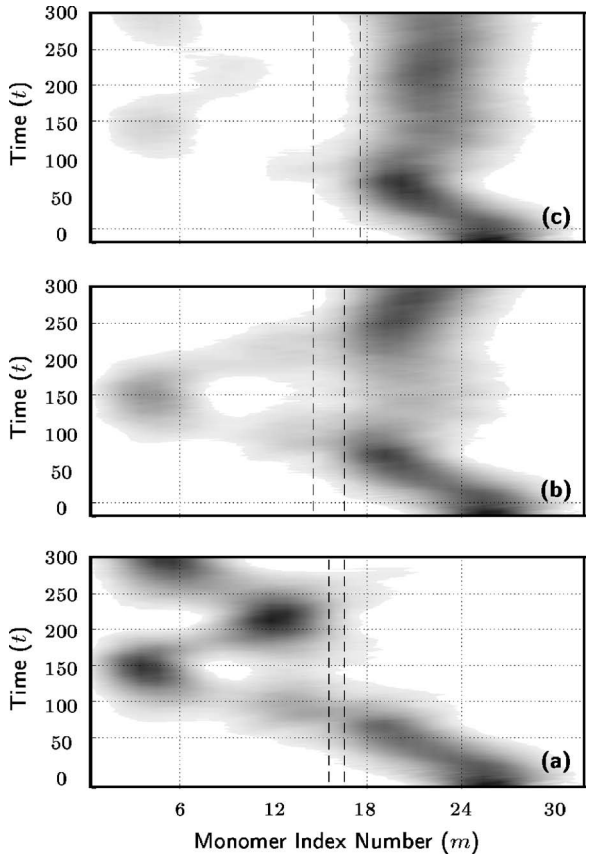

FIG. 5. The time evolution of the density of charge at $E_0=5.0\times10^4$ V/cm in systems of $N=31$ phenylene rings, where in (a)–(c) the torsion angle of the one, two, and three center most phenylene rings within the region enclosed by the dashed lines have been set to 15° in otherwise completely planar systems.

that of systems where only the single center most phenylene ring has been twisted by 21.3° and 26.1°, respectively, i.e., by angles φ such that the reduction in resonance integral, $\delta\beta(\varphi)=\beta(0°)[1-\cos(\varphi)]$, caused by the single ring torsion exactly equals that of integer multiples $\eta=[2,3]$ of $\delta\beta(\varphi)$. It is therefore the sum rather than the parts of reduction of local resonance integrals that ultimately decides the characteristics of the transport dynamics. This explains why the charge carrier ceases to propagate further than the 12th phenylene ring in the system of Fig. 4(e).

The effect of increasing the barrier height is thus strongly coupled to that of increasing the barrier width. We have performed studies in which the torsion angle of the single center most phenylene ring in otherwise completely planar systems was set to 10°, 20°, 30°, and 40°. The polaron motion with increasing torsion angle shows a transition from adiabatic transport into a situation with localized states between torsion angles of 20° and 30° in close correspondence with the discussion above concerning the relation between the barrier height and the barrier width.

The empirical relationship deduced above for analyzing the characteristics of chains with phenylene ring torsion as the sum of the local resonance integral modulation is not a general relation for combination of single ring torsion barriers. If, for example, two twisted phenylene rings are gradu-

ally shifted away from each other in the otherwise planar system, we find that at some distance the torsion of the second ring will not affect the dynamics of the polaron traversing the first torsion barrier. For $E_0=5.0\times10^4$ V/cm, the distance amounts to 7 monomer units of PPV. In the process of crossing the region of the first ring with nonzero torsion, the polaron does of course lose momentum and is therefore not able to traverse also the barrier constituted by the second twisted phenylene ring.

IV. SUMMARY AND DISCUSSION

We have developed a three-dimensional SSH-type model which enables detailed investigations of the dependence of intrachain charge-carrier dynamics on ring torsion in π-conjugated systems, in our case PPV. In particular, we have studied the problem of electron localization caused by random variations in the torsion angles and the transition from adiabatic to nonadiabatic intrachain polaron transport. As a basis for the studies of disordered systems, we first explored the impact of uniform phenylene ring torsion. The observed mobility has a $\cos^2(\varphi_0)$ dependence on the torsion angle. Since the resonance integral $\beta_n \propto \cos(\varphi_0)$, this implies that $\mu \propto \beta^2$. Thus, for small torsion angles in a uniform distribution, the effect on the polaron mobility is very small.

This situation changes dramatically when the torsion angles vary randomly along the PPV chain. For a rectangular distribution of $\{\varphi_n\}$ on intervals $[0,\varphi_u]$, we observe electron localization and a field-induced transport process. The zero-field mobility is essentially zero for values of φ_u as small as 5°. By increasing the field strength, the tunneling barriers are reduced and a crossover to an adiabatic transport process is observed, but with a reduced mobility as compared to the planar reference system. This crossover occurs at higher and higher field strengths for increasing values of φ_u, e.g., for $\varphi_u=20°$, the adiabatic transport is absent even for field strengths as large as $E_0=5.0\times10^4$ V/cm.

We also present results from simulations performed for steplike changes in the value of φ_n for which quantitative details concerning the transition from adiabatic to nonadiabatic transport are obtained. It is clear from these simulations that a change (increase) in torsion angle results in a barrier for adiabatic transport. The strength of the barrier depends on the magnitude and the extension of the region with larger torsion angles. For small torsion angles and short barrier extensions, it is the sum of the decrease in the resonance integrals of the individual rings that produces the strength of the total barrier.

The results presented above show that in most cases, polaron transport along a single polymer chain is nonadiabatic in the limit of zero applied field. Any finite random fluctuation in the torsion angle will lead to this result. The relative weakness of the barriers indicate, however, that a crossover to adiabatic transport is possible. As discussed above, this can be achieved by increasing the electric-field strength. The barriers we generate at 5°–10° torsion can be surpassed at a field strength of $E_0=5.0\times10^4$ V/cm. Assuming an effective length of the barrier of the order of the length of the phenylene ring, i.e., 3–4 Å, the field-induced potential energy drop across this regions is approximately 2 meV. Thus, the barriers that are surpassed for this field strength are of the order of a few meV. Replacing the potential-energy drop caused by the external field with an activation energy from a phonon heat bath indicated that these barriers are easily overcome at room temperature. Thus, for distributions of torsion angles not exceeding 5°–10°, we can expect relatively high room-temperature intrachain mobilities. For larger torsion angles, however, the barriers are considerably higher which results in low mobility with strong temperature dependence. This difference corresponds very well to the difference between poly(9, 9-dioctylfluorene) (PFO) and poly[2-methoxy, 5-(2′-ethyl-hexyloxy)-1, 4-phenylene vinylene] (MEH-PPV) discussed above.

ACKNOWLEDGMENT

Financial support from the Center of Organic Electronics (COE), Swedish Foundation of Strategic Research, is gratefully acknowledged.

*Electronic address: mahul@ifm.liu.se
†Electronic address: sst@ifm.liu.se

[1] N. Karl, Synth. Met. **133-134**, 649 (2003).
[2] J. L. Bredas, D. Beljonne, V. Coropceanu, and J. Cornil, Chem. Rev. (Washington, D.C.) **104**, 4971 (2004).
[3] A. Troisi and G. Orlandi, J. Phys. Chem. B **109**, 1849 (2005).
[4] A. Troisi and G. Orlandi, Phys. Rev. Lett. **96**, 086601 (2006).
[5] M. Redecker, D. D. C. Bradley, M. Inbasekaran, and E. P. Woo, Appl. Phys. Lett. **73**, 1565 (1998).
[6] I. H. Campbell, D. L. Smith, C. J. Neef, and J. P. Ferraris, Appl. Phys. Lett. **74**, 2809 (1999).
[7] Z. G. Yu, D. L. Smith, A. Saxena, R. L. Martin, and A. R. Bishop, Phys. Rev. Lett. **84**, 721 (2000).
[8] W. P. Su, J. R. Schrieffer, and A. J. Heeger, Phys. Rev. B **22**, 2099 (1980).
[9] Å. Johansson and S. Stafström, Phys. Rev. B **68**, 035206 (2003).
[10] S. Lifson and A. Warshel, J. Chem. Phys. **49**, 5116 (1968).
[11] R. S. Mulliken, J. Chem. Phys. **46**, 675 (1949).
[12] A. Hansson and S. Stafström, Phys. Rev. B **67**, 075406 (2003).
[13] R. S. Mulliken, C. A. Reike, D. Orloff, and H. Orloff, J. Chem. Phys. **17**, 1248 (1949).
[14] M. N. Bussac, J. D. Picon, and L. Zuppiroli, Europhys. Lett. **66**, 392 (2004).
[15] T. Holstein, Ann. Phys. **8**, 343 (1959).
[16] M. Hultell and S. Stafström, Chem. Phys. Lett. **428**, 446 (2006).
[17] A. A. Johansson and S. Stafström, Phys. Rev. B **69**, 235205 (2004).
[18] A. Miller and E. Abrahams, Phys. Rev. **120**, 745 (1960).